

Synthesis and electrochemical polymerization of a novel 2-(thiophen-2-yl)-4-(thiophen-2-ylmethylene)oxazol-5(4H)-one monomer for supercapacitor applications



Evrım Hür^{a,*}, Andaç Arslan^a, Deniz Hür^{b,c}

^a Eskişehir Osmangazi University, Department of Chemistry, Faculty of Arts and Science, 26480 Eskişehir, Turkey

^b Anadolu University, Science Faculty, Department of Chemistry, 26470 Eskişehir, Turkey

^c Anadolu University, Plant, Drug and Scientific Researches Center (AÜBİBAM), 26470 Eskişehir, Turkey

ARTICLE INFO

Article history:

Received 16 June 2015

Received in revised form 9 November 2015

Accepted 8 December 2015

Available online 11 December 2015

Keywords:

Thiophene

Conducting polymers

Organic synthesis

Electrode materials

Supercapacitor

ABSTRACT

In this study, the organic synthesis, electrochemical polymerization and electrochemical characterization of a novel 2-(thiophen-2-yl)-4-(thiophen-2-ylmethylene)oxazol-5(4H)-one, **3**, monomer have been reported for supercapacitor applications. Electrode active material was formed electrochemically coating of poly(2-(thiophen-2-yl)-4-(thiophen-2-ylmethylene)oxazol-5(4H)-one) (PTTMO) on pencil graphite electrode (PGE). Electrochemical polymerization was carried out by chronoamperometric (CA) technique in an acetonitrile (ACN) solution containing 0.01 M monomer and 0.10 M tetrabutylammonium perchlorate (TBAP). The prepared PGE/PTTMO electrode has been monitored by scanning electron microscopy (SEM). Electrochemical properties of the electrode have been investigated by CV, electrochemical impedance spectroscopy (EIS), galvanostatic charge–discharge and repeating chronopotentiometry (RCP) techniques with two or three electrode systems. PGE/PTTMO has exhibited a capacitive performance with highest specific capacitances of 193.00 F g⁻¹ at a scan rate of 10 mV s⁻¹. On the other hand, the electrode has shown good charge–discharge cycling stability with the retained ratio about 90.83%.

© 2015 Elsevier B.V. All rights reserved.

1. Introduction

Nowadays, energy storage and alternative energy storage systems have great importance due to the depletion fossil fuels and the demand for environmental friendly energy storage systems [1,2]. Among the various energy storage systems, supercapacitors also known as electrochemical capacitors, represent the most promising electrochemical systems for energy storage because of their several advantages such as high power density, fast charging–discharging rate, cycling stability and low cost. These properties allow supercapacitors to fill the gap between traditional capacitors and batteries [3–6]. According to charge-storage mechanism, supercapacitors can be divided into two types: Electrochemical double layer capacitors and redox supercapacitors (pseudocapacitors). Supercapacitors store and release energy based on one of combination of these mechanisms, depending on the nature of the used electrode materials [7]. The energy storage of electrochemical double layer capacitors is the separation of the electronic and ionic charges at the interface between electrode materials and the electrolyte solution. Carbon-based materials such as carbon nanotube, active carbon and graphene are most widely used as an electrode active material in electrochemical double layer capacitors because of their high surface

area and excellent stability. However, their low specific capacitances restrict the applications of carbon-based materials for supercapacitors [8,9]. In pseudocapacitors, energy storage is based on fast and reversible redox faradaic reactions which occur within the active materials of electrodes. The active electrode materials used for pseudocapacitors are metal oxides and electrically conducting polymers [10]. Especially, electrically conducting polymers have been considered as an ideal candidate for pseudocapacitors because of their good electrical conductivity, large specific capacitance, easy synthesis and low cost. Although electrically conducting polymers provide these advantages, they suffer from the poor cycling stability during long charge–discharge processes [11–13]. Therefore, electrically conducting polymers have been combined with carbon-based materials to use as electrode active material for supercapacitor applications. Among conducting polymers, polythiophene and its derivatives have been extensively studied for supercapacitor electrodes [11,14–17]. In recent years, to improve the electrochemical energy storage properties and to enhance the specific capacitances, these polymers have been modified with the organic molecules [18–26].

In our previous works [16,17], polythiophene and its derivatives were characterized on PGE for supercapacitor applications and the highest specific capacitance value of 131.99 F g⁻¹ were obtained for the electrode which formed using poly(3-methylthiophene). In this work, in order to present a new electrode active material and to obtain

* Corresponding author.

E-mail address: evrimhur@ogu.edu.tr (E. Hür).

higher specific capacitance values, we report the synthesis, electro-polymerization and electrochemical characterization of a novel 2-(thiophen-2-yl)-4-(thiophen-2-ylmethylene)oxazol-5(4 H)-one, **3**, monomer on PGE. The synthesis of this new thiophene monomer has been realized differently from the literature by using benzotriazole chemistry. Benzotriazole, which is a considerable heterocyclic compound, has advantages (i.e. be stability in many synthesis conditions, nontoxic, inexpensive and easy to remove at the end of the synthesis in both acidic and basic media) in the development of new synthesis methods. Since benzotriazole and its derivatives are UV-active, their reaction process is visualized easily. On the other hand, most of benzotriazole derivative has crystalline structure that enables to examine with chromatographic methods [27]. The monomer, **3**, has been electrochemically polymerized on PGE by using CA technique. Then, the prepared electrode has been characterized by using SEM, CV, EIS and RCP techniques. Real supercapacitor performance of the electrode has been examined by using galvanostatic charge–discharge in two electrode system.

2. Experimental

2.1. Chemicals and materials

All chemicals were of reagent-grade purity or better, and used as obtained from the commercial suppliers. THF was used freshly after distillation with sodium in the presence of benzophenon. Column chromatography was conducted with silica gel 200–425 mesh. NMR spectra were recorded in CDCl_3 with TMS as the internal standard for ^1H (500 MHz) or a solvent as the internal standard for ^{13}C (125 MHz) using Bruker NMR equipment. All electrochemical experiments except galvanostatic charge–discharge method were carried out in a conventional three electrode system using PGE as working electrode, platinum sheet as a counter electrode and pseudo Ag wire as a reference electrode, which all potentials were referenced. PGE is Tombo lead with a diameter of 0.50 mm. The PGE has been prepared by cutting the leads into 3 cm long sticks and 2 cm (area 0.31 cm^2) was dipped in electrolyte. A Rotring Tikky pencil model was used as a holder for PGE. Electrical contact with the PGE was obtained by soldering a metallic wire to the metallic part of the holder. All electrodes were cleaned in ACN using ultrasonic bath (Bandelin Sonarex) and dried before each experiment. The all electrochemical measurements were carried out using A Gamry 3000 potentiostat/galvanostat/ZRA system and obtained data were analyzed using Gamry CMS-300 (version 5.50b) framework/analysis software. All electrochemical experiments were carried out at 25 °C and at open air atmosphere. Surface morphology was studied using a Zeiss Ultraplus model field emission scanning electron microscopy (FE-SEM).

2.2. Synthesis of 2-(thiophen-2-yl)-4-(thiophen-2-ylmethylene)oxazol-5(4 H)-one, **3**

2-(thiophen-2-yl)-4-(thiophen-2-ylmethylene)oxazol-5(4 H)-one, **3**, was synthesized described method in Scheme 1 [28,29].

2.2.1. Preparation of (1 H-benzo[d][1,2,3]triazol-1-yl)(thiophen-2-yl)methanone, **1**

To a solution of 1 H-benzotriazole (4 eq.) in THF (80 mL), SOCl_2 (1 eq.) was added dropwise with stirring at room temperature. After

30 min, a solution of thiophene-2-carboxylic acid (1 eq.) was added. After 2 h, the solid was filtered and washed with THF (50 mL). The solvent was removed under vacuum from the combined filtrate. To the residue, ethyl acetate (50 mL) was added; the mixture was washed with 20% Na_2CO_3 (3×30 mL). The organic layer was dried over anhydrous Na_2SO_4 , then it was filtered and the solvent was evaporated under vacuum to obtain a solid product, (1 H-benzo[d][1,2,3]triazol-1-yl)(thiophen-2-yl)methanone, **1**, in 90% yield.

2.2.2. Preparation of 2-(thiophene-5-carboxamido)acetic acid, **2**

The solution of (1 H-benzo[d][1,2,3]triazol-1-yl)(thiophen-2-yl)methanone, **1**, (1 eq.) in dioxane (80 mL) was added to solution of 2-aminoacetic acid (1 eq.) in distilled water (40 mL) and NaOH (1 eq.). After 2 h, dioxane was removed under vacuum and the resulted reaction mixture was washed with ethyl acetate (3×30 mL). Collected water layers were acidified to pH = 2 using 10% HCl solution. This solution was extracted with ethyl acetate (2×30 mL). Collected organic layers were dried over anhydrous Na_2SO_4 , and the solvent was removed under vacuum to obtain a solid product 2-(thiophene-5-carboxamido)acetic acid, **2**, in 97% yield.

2.2.3. Preparation of 2-(thiophen-2-yl)-4-(thiophen-2-ylmethylene)oxazol-5(4 H)-one, **3**

2-(thiophene-5-carboxamido)acetic acid (1 eq.), thiophene-2-carbaldehyde (1 eq.) and sodium acetate (1 eq.) in acetic anhydride (10 mL) was heated to reflux for 2 h. Then the solvent was evaporated under vacuum to give the crude product, which was purified by column chromatography to obtain pure product 2-(thiophen-2-yl)-4-(thiophen-2-ylmethylene)oxazol-5(4 H)-one, **3**, in 93% yield.

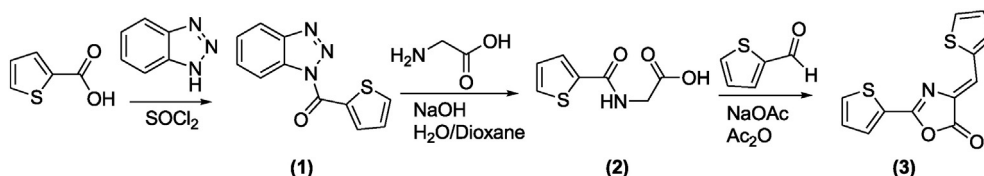
2-(thiophen-2-yl)-4-(thiophen-2-ylmethylene)oxazol-5(4H)-one, 3. (93%), yellow microcrystals, ^1H NMR (CDCl_3 , 500 MHz) 7,90 (d, $J = 3,08$ Hz, 1H), 7,33 (d, $J = 5,04$ Hz, 1H), 7,70 (d, $J = 4,31$ Hz, 1H), 7,64 (d, $J = 3,62$ Hz, 1H), 7,46 (s, 1H), 7,23 (t, $J = 4,05$ Hz, 1H), 7,18 (t, $J = 3,91$ Hz, 1H); ^{13}C NMR (CDCl_3 , 125 MHz) δ 124,1, 128,0, 128,6, 128,7, 130,6, 132,6, 133,1, 134,7, 135,14, 137,7, 158,3, 166,6 ppm.

2.3. Preparation of the electrode

Electrode was prepared by electrochemical polymerization of 2-(thiophen-2-yl)-4-(thiophen-2-ylmethylene)oxazol-5(4 H)-one, **3**, on PGE using CA technique in ACN solution containing 0.01 M monomer and 0.10 M TBAP. CA experiments were performed applying a constant potential of +1.50 V for 240 s. After the electrochemical polymerization, PGE/PTTMO was removed from the polymerization medium and rinsed with ACN to remove monomer molecules and then dried in air. The mass of the polymer film was measured by weighing using a precision balance after being held under reduced pressure.

2.4. Electrochemical characterization

Electrochemical performances of PGE and PGE/PTTMO were tested by using CV, EIS, galvanostatic charge–discharge and RCP techniques in monomer free solution. CV measurements were employed in the potential range between -0.20 and $+1.90$ V at different scan rates (10, 20, 30, 50 and 75 mV s^{-1}). The specific capacitance of PGE/PTTMO was calculated at all scan rates from CV measurements using following



Scheme 1. Preparation of 2-(thiophen-2-yl)-4-(thiophen-2-ylmethylene)oxazol-5(4 H)-one, **3**.

equation:

$$C_s = \frac{I}{(dV/dt)m} \quad (1)$$

where “ I ” is the average current, “ dv/dt ” is the scan rate and “ m ” is the deposited weight of polymer film [30].

The electrochemical impedance spectra were recorded at an open circuit potential (OCP) which was measured before the each measurement in the frequency ranged from 10^5 to 10^{-2} Hz with ac-voltage amplitude of 10 mV. The specific capacitances of the electrodes were calculated from EIS measurements using following equation at a low frequency range between 10^{-2} and 10^{-1} Hz:

$$C_s = -\frac{1}{2\pi f Z_{im} m} \quad (2)$$

where “ f ”, “ Z_{im} ” and “ m ” are the frequency, imaginary part of the total complex impedance and the deposited weight of polymer film, respectively [31].

Galvanostatic charge–discharge measurements were carried out to reveal the charge–discharge profiles of the electrodes in two-electrode system at the current of 0.1 mA in the potential range between 0.00 and +1.50 V. The specific capacitance, energy density (E), power density (P) and coulombic efficiency (η) of the electrodes were calculated from the discharge curves using following equations:

$$C_s = 2 \frac{I \Delta t_d}{\Delta V m} \quad (3)$$

$$E = \frac{1}{2} C_s (\Delta V)^2 \quad (4)$$

$$P = \frac{E}{\Delta t_d} \quad (5)$$

$$\eta = \frac{\Delta t_d}{\Delta t_c} \times 100 \quad (6)$$

where “ I ” is the discharge current, “ Δt_c ” and “ Δt_d ” is the time of charging and discharging, “ ΔV ” is the potential range during the discharge and “ m ” is the deposited weight of polymer film [32,33].

RCP measurements were realized by applying a double current pulse (± 2 mA) during 25 s for 1000 consecutive cycles to investigate the long term charge–discharge cycling stabilities of the electrodes.

3. Results and discussion

3.1. Preparation of the electrode

PGE/PTTMO was prepared by forming PTTMO on PGE using CA technique in ACN solution containing 0.01 M monomer and 0.10 M TBAP. The optimization measurements were employed to determine the effect of the applied potential and time on the preparation of the electrodes. PTTMO films were grown on PGE applying different constant potentials of +1.20, +1.30, +1.40, +1.50 and +1.60 V over the same time interval (300 s). Single cycle voltammograms of the electrodes in the potential range between -0.20 and $+1.90$ V at 30 mV s^{-1} were recorded in monomer free solution (Fig. 1a). The anodic peak current was found to increase with increasing potential up to +1.50 V. Then, the potential was held constant for different times (180, 240, 300, 360 and 420 s). Single cycle voltammograms of the electrodes were recorded at the same conditions and the highest current was obtained for 240 s (Fig. 1b). As the thickness of the film increases, the polymer film becomes relatively low electrically conductive that leads to higher resistance and more difficult deposition after 240 s. Thus, optimum CA conditions for the preparation of PGE/PTTMO are +1.50 V potential

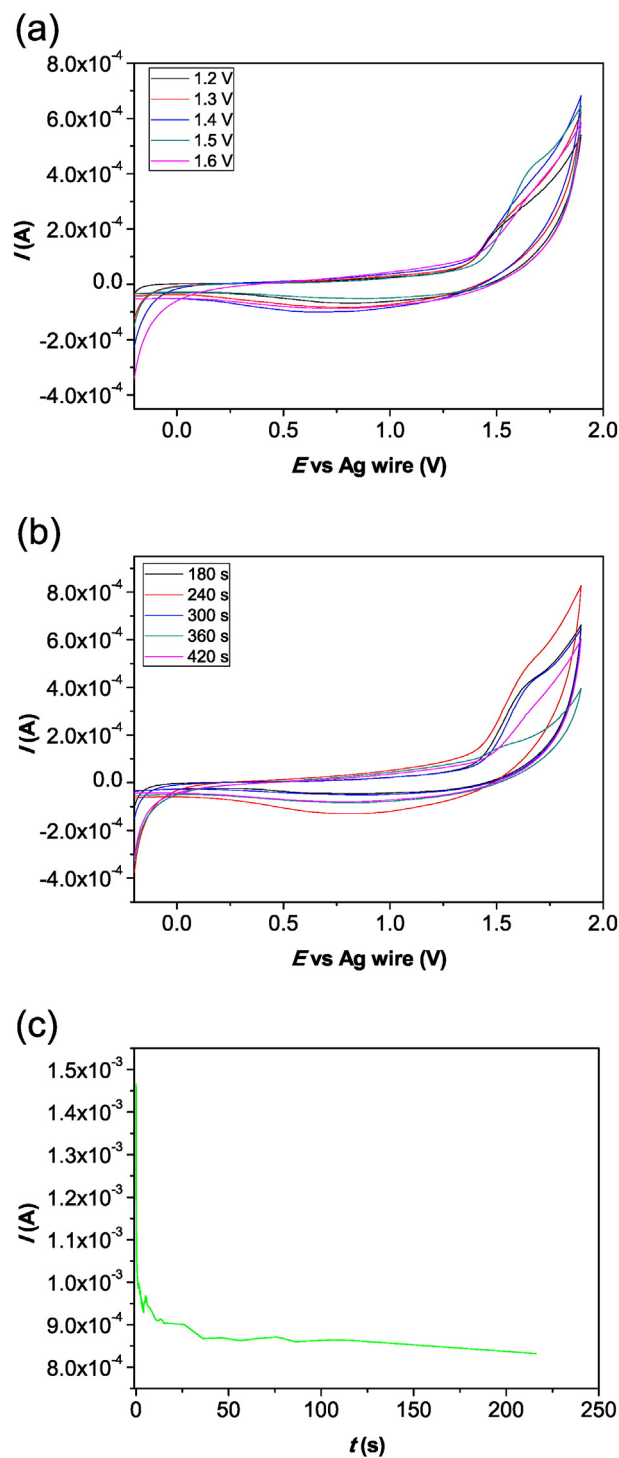


Fig. 1. Single cycle voltammograms of PGE/PTTMO which are prepared (a) by applying different constant potentials for 300 s and (b) by applying +1.50 V of constant potential for different times. (c) Chronoamperogram of growth of PTTMO on PGE in ACN solution containing 0.01 M 2-(thiophen-2-yl)-4-(thiophen-2-ylmethylene)oxazol-5(4H)-one and 0.10 M TBAP. Applied potential: +1.5 V, time: 240 s.

and 240 s time. Chronoamperogram that belongs to synthesis of PTTMO film on PGE is shown in Fig. 1c. The current decreased sharply at the beginning due to electrochemical adsorption of 2-(thiophen-2-yl)-4-(thiophen-2-ylmethylene)oxazol-5(4H)-one, **3**, on PGE. Then, current remained relatively stable. These results indicate the formation of PTTMO film on PGE [34–36].

3.2. Surface morphology of the electrodes

SEM micrographs of the electrodes were taken to monitor the surface morphology of PGE and PGE/PTTMO (Fig. 2). As can be seen from Fig. 2a, PGE, which showed the presence of regularly ordered graphite layers, has relatively rough and porous structure. It can be clearly seen that the surface of PGE is significantly changed when covered with PTTMO. PGE/PTTMO consists of irregular spread PTTMO sheets with different sizes (Fig. 2b). Although such structures are unfavorable for supercapacitor applications, they might provide more accessible internal surface area within its spread sheets for electrolyte ions during electrochemical processes.

3.3. Electrochemical characterization of the electrodes

To examine PGE and PGE/PTTMO as electrode active materials, capacitive properties of the electrodes were investigated by means of CV, EIS, galvanostatic charge–discharge and RCP measurements in monomer free solution.

3.3.1. Cyclic voltammetry studies

The obtained voltammograms from CV measurements were used to study the effect of scan rate on the specific capacitance of the electrode in the potential range between -0.20 and $+1.90$ V. Fig. 3a shows the cyclic voltammograms of PGE and PGE/PTTMO recorded at a scan rate of 10 mV s^{-1} . As can be seen from Fig. 3a, PGE/PTTMO exhibits a larger current response when compared to PGE in the same electrolyte at a scan rate of 10 mV s^{-1} . This indicates that the surface area of PGE/PTTMO is larger than PGE and it leads to an enhancement of charge

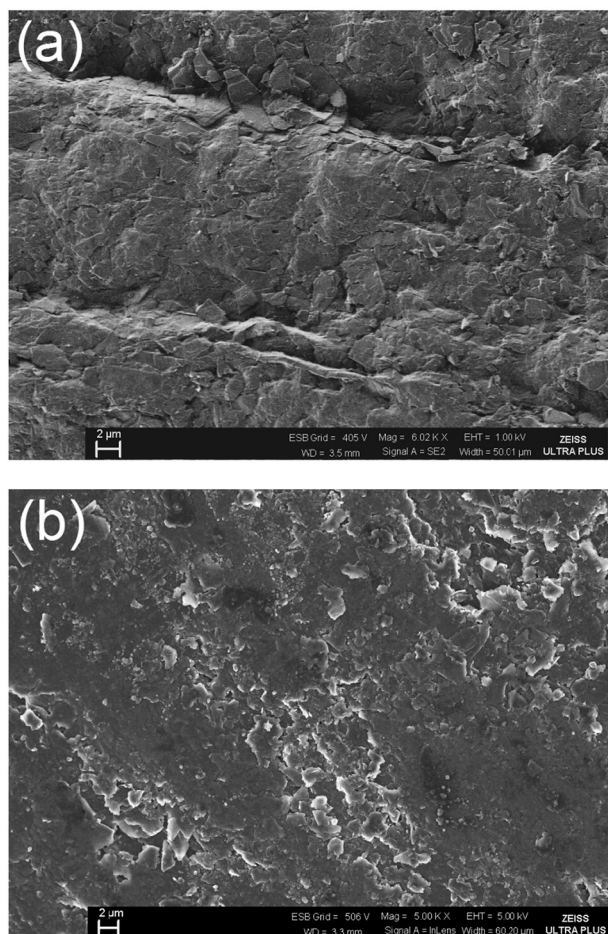


Fig. 2. SEM images of (a) PGE and (b) PGE/PTTMO.

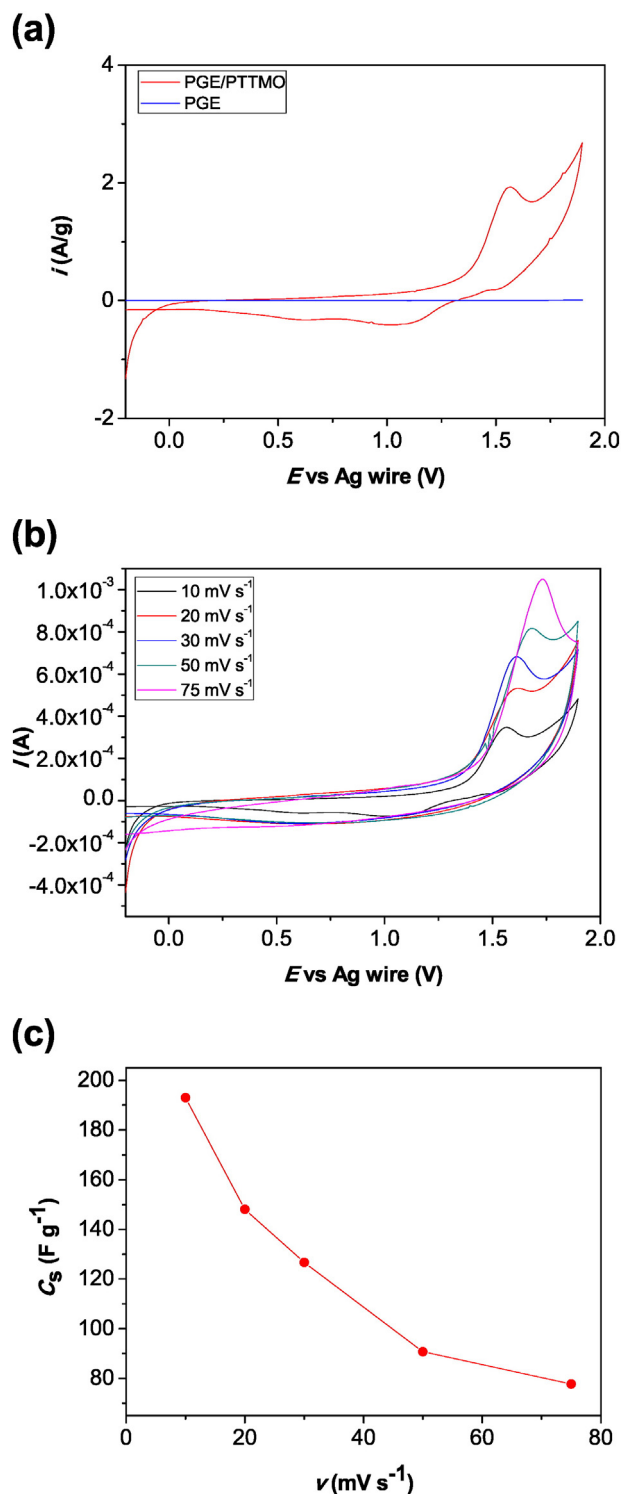
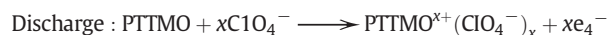
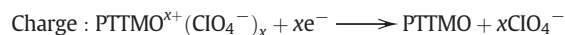


Fig. 3. (a) CV curves of PGE and PGE/PTTMO at a scan rate of 10 mV s^{-1} . (b) CV curves of PGE/PTTMO at different scan rates. (c) Variation of the specific capacitance values of the electrodes with scan rates.

storage capability of PGE. On the other hand, rectangular shape of CV curve is characteristic of ideal electrical double layer capacitance mechanism. It can be seen from Fig. 3a, the shape of CV curve of the PGE/PTTMO deviates from the rectangular shape. Redox peaks formed on CV curve are a result of redox processes such as the oxidation and reduction of the polymer backbone [37]. Fig. 3b gives the cyclic voltammograms of PGE/PTTMO at different scan rates of $10, 20, 30, 50$ and 75 mV s^{-1} . The specific capacitances of the electrode were calculated

by the current of CV curves at all scan rates using Eq. (1) and were plotted versus scan rates (Fig. 3c). The highest specific capacitance of the electrode was found to be as 193.00 F g^{-1} at a scan rate of 10 mV s^{-1} . On the other hand, the specific capacitance of PGE/PTTMO is higher than that of PGE (0.31 F g^{-1}) at the same scan rate. The specific capacitance of the electrode varies inversely proportional to scan rate. This is a result of the partly inaccessibility of the surface of the electrodes at high scan rates. During oxidation–reduction process, electron exchange takes place at electrode/electrolyte interface, as shown in the following equations:



As scan rates increase, the rate of migration and orientation of the electrolyte ions are limited in the electrolyte. Therefore, electrolyte ions only reach to the outer surfaces of the electrode. This leads to decrease in the capacitance [38–42].

3.3.2. Electrochemical impedance spectroscopy studies

Although results of EIS are generally smaller than that of CV and galvanostatic charge–discharge measurements, it is a principal method to characterize the frequency response of electrode materials for supercapacitor [43]. EIS measurements were employed at an open circuit potential (OCP) in the frequency ranged from 10^5 to 10^{-2} Hz with ac-voltage amplitude of 10 mV. OCP values of the electrode measured before the each experiment for 1200 s was determined as +0.90 and +0.14 V for PGE/PTTMO and PGE. Nyquist plots of the electrodes are given in Fig. 4a and b. Nyquist plots of electrodes for supercapacitors are divided into two regions: (i) semicircle at high frequencies which is combination of charge transfer resistance and double layer capacitance at polymer film/electrolyte interface and (ii) vertical line at low frequencies which is characteristic of the diffusion controlled process in the electrolyte indicating faradaic process [33,44,45]. In Fig. 4b, it can be obviously seen that there is a semicircle and vertical line at high and low frequency region, respectively. This confirms the energy storage mechanism of PGE/PTTMO which is based on electrochemical double layer capacitance and pseudocapacitance mechanism. PGE has just a straight line at scanned frequencies. It reveals that PGE shows low charge transfer resistance with a vertical line towards lower frequency, demonstrating an ideal electrochemical double layer capacitor. The specific capacitances of the electrodes can be calculated from EIS measurements by Eq. (2). Therefore, $1/(2\pi f)$ versus Z_{im} can be plotted and the reciprocal of slope of the plot gives the capacitance [46]. Since the majority of the capacitance of the electrodes is only available at low frequencies [31], values of $1/(2\pi f)$ were plotted versus Z_{im} for low frequency region between 10^{-2} and 10^{-1} Hz and the plots are given in Fig. 4c. The specific capacitances of PGE/PTTMO and PGE were calculated as 12.12 and $6.13 \times 10^{-3} \text{ F g}^{-1}$, respectively.

3.3.3. Galvanostatic charge–discharge studies

Real supercapacitor performances of the electrodes were evaluated by galvanostatic charge–discharge measurements at a current of 0.1 mA in the potential ranged from 0.00 to +1.50 V in two-electrode system with identical electrodes. Fig. 5 shows the charge–discharge profiles of the electrodes. It is observed that the charge–discharge curves of PGE/PTTMO deviated from the typical linear curve. This indicates the pseudocapacitive character at this voltage range [47]. Voltage drop (IR drop) at the initiation of the discharge was obtained as 0.02 and 0.08 V for PGE/PTTMO and PGE, respectively. IR drop of PGE/PTTMO is much lower than that of PGE, indicating the less energy loss due to internal resistance of PTTMO [48]. C_s , E , P and η of the electrodes were calculated by Eqs. (3), (4), (5) and (6), respectively and were given in Table 1. It is known that the duration of one full charge–discharge cycle becoming longer is indicative for higher capacitance [49]. The durations of one

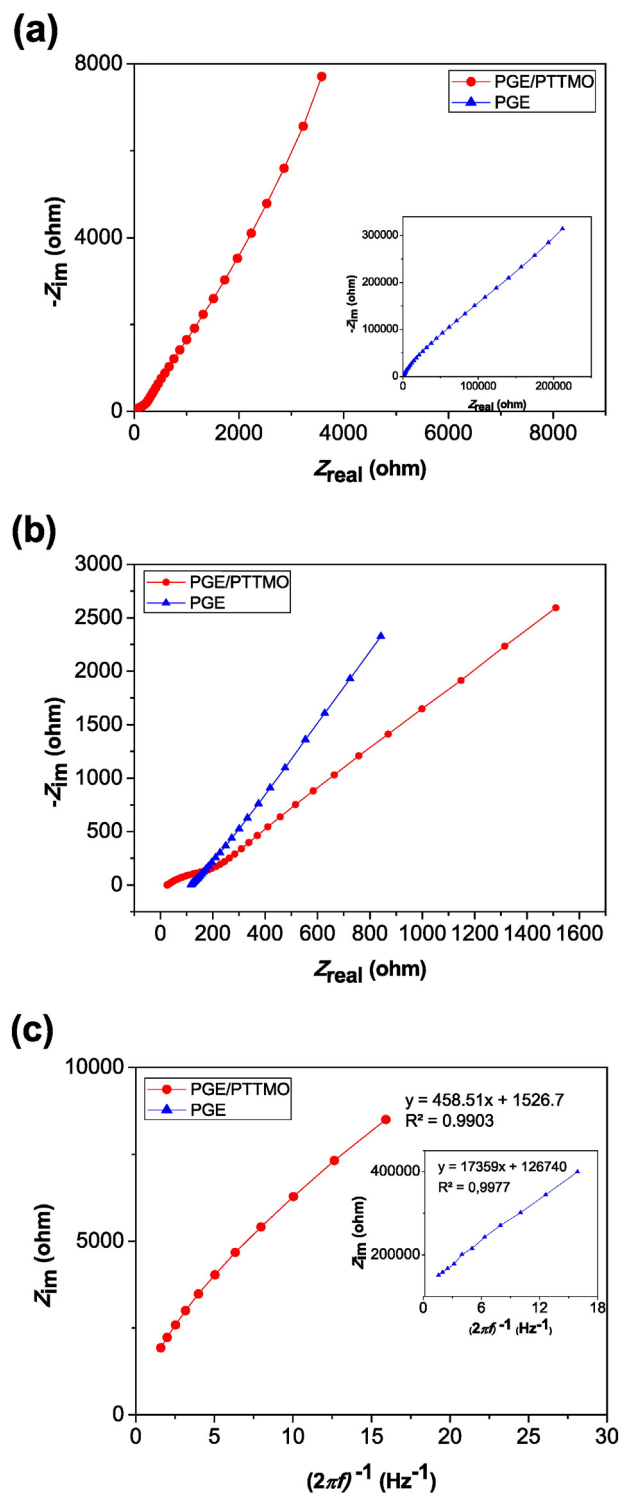


Fig. 4. (a) Nyquist plots of the electrodes at open circuit potential in ACN solution containing 0.10 M TBAP. Inset: Nyquist plots of uncoated PGE at open circuit potential in ACN solution containing 0.10 M TBAP. (b) Enlarged version of low-resistance state of Nyquist plots of the electrodes at open circuit potential in ACN solution containing 0.10 M TBAP. (c) The linear relations between Z_{im} between $1/(2\pi f)$ for the electrodes.

full charge–discharge cycle are ranged as $t_{d, \text{PGE/PTTMO(CA)}} > t_{d, \text{PGE}}$. The discharge specific capacitances of PGE/PTTMO and PGE were calculated to be 145.26 and 0.04 F g^{-1} , respectively, which have similar trend with the results obtained from CV and EIS measurements. On the other hand, coulombic efficiency of PGE can be enhanced by the formation PTTMO on PGE.

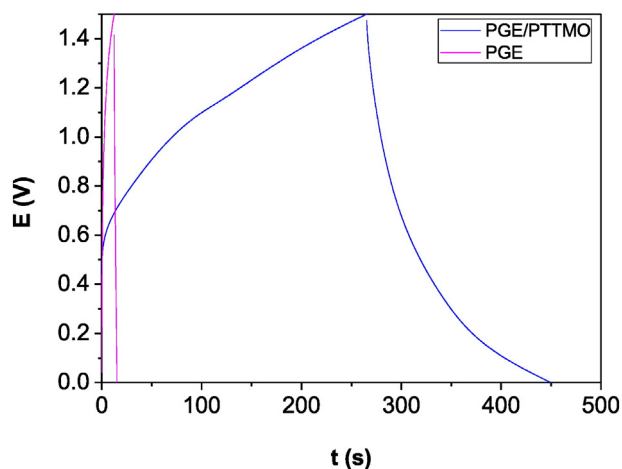


Fig. 5. Galvanostatic charge–discharge curves for supercapacitor in two-electrode system.

3.3.4. Repeating chronopotentiometry studies

In order to test the long term charge–discharge cycling stability of the electrodes, RCP measurements were employed applying double current pulse (± 2.0 mA) during 25 s for 1000 cycles. Fig. 6a and b represent first 5 and last 5 cycle charge–discharge behaviors of the electrodes in 1000 cycle charge–discharge tests. It can be observed that PGE/PTTMO and PGE reach to charge cut-off potential of 2.18 and 1.98 V at first cycle, respectively. The variation of the charge cut-off potential values of the electrodes versus number of charge–discharge cycles are given in Fig. 6c. PGE/PTTMO and PGE retained about 90.83 and 80.80% of initial charge cut-off potential after 1000 cycles, respectively.

4. Conclusions

In this study, a novel thiophene-based monomer 2-(thiophen-2-yl)-4-(thiophen-2-ylmethylene)oxazol-5(4H)-one, **3**, was successfully prepared for the first time and it was electropolymerized on PGE by electrochemical technique. SEM micrographs confirm the formation of PTTMO films on PGE surface. PGE and PGE/PTTMO were characterized as electrode materials for supercapacitor by using CV, EIS, galvanostatic charge–discharge and RCP techniques in ACN solution which contains 0.10 M TBAP. Electrochemical measurements confirm the successful formation of PTTMO film onto the PGE surface. Specific capacitance values of PGE/PTTMO calculated by CV, EIS and galvanostatic charge–discharge techniques are higher than that of PGE. PGE/PTTMO exhibited the maximum specific capacitances of 193.00 F g^{-1} at a scan rate of 10 mV s^{-1} . Furthermore, the electrode showed charge–discharge cycling stability with the retained ratios about 90.83%. Our results showed that PGE/PTTMO is promising electrode material for supercapacitor applications.

Acknowledgments

This work was supported by Eskişehir Osmangazi University Research Found (Project No: 2014-418). The authors would like to thank Dr. Müjdat Çağlar and Seval Aksoy for SEM. The authors would also like to thank AÜBİBAM for the NMR analysis.

Table 1

C_s , E , P and η values of the electrodes calculated from galvanostatic charge–discharge curves.

Electrodes	$C_s/\text{F g}^{-1}$	$E/\text{kWh kg}^{-1}$	$P/\text{kW kg}^{-1}$	$\eta/\%$
PGE/PTTMO	145.26	144.19	0.78	69.40
PGE	0.04	0.04×10^{-3}	0.014×10^{-3}	23.16

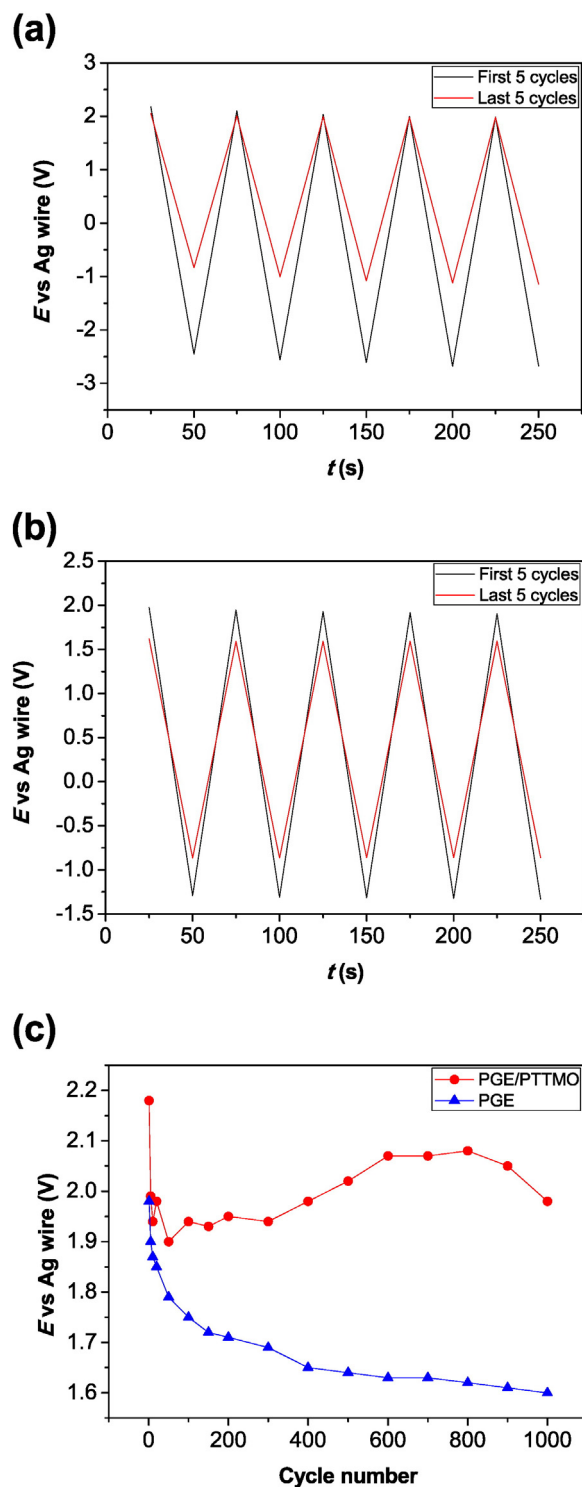


Fig. 6. First 5 and last 5 cycles charge–discharge behaviors of (a) PGE/PTTMO and (b) PGE in 1000 cycles charge–discharge tests in ACN solution containing 0.10 M TBAP. (c) Variation of the charge cut-off potential of the electrodes versus number of charge–discharge cycles.

References

- [1] Y. Hou, L. Chen, L. Zhang, J. Kiang, T. Fujita, J. Jiang, M. Chen, Ultrahigh capacitance of nanoporous metal enhanced conductive polymer pseudocapacitors, *J. Power Sources* 225 (2013) 304–310.
- [2] P. Zhao, W. Li, G. Wang, B. Yu, X. Li, J. Bai, Z. Ren, Facile hydrothermal fabrication of nitrogen-doped graphene/Fe₂O₃ composites as high performance electrode materials for supercapacitor, *J. Alloys Compd.* 604 (2014) 87–93.

- [3] A.G. Pandolfo, A.F. Hollenkamp, Carbon properties and their role in supercapacitors, *J. Power Sources* 157 (2006) 11–27.
- [4] Z. Gao, F. Wang, J. Chang, D. Wu, X. Wang, X. Wang, F. Xu, S. Gao, K. Jiang, Chemically grafted graphene-polyaniline composite for application in supercapacitor, *Electrochim. Acta* 133 (2014) 325–334.
- [5] J. Yang, L. Lian, H. Ruan, F. Xie, M. Wei, Nanostructured porous MnO₂ on Ni foam substrate with a high mass loading via a CV electrodeposition route for supercapacitor application, *Electrochim. Acta* 136 (2014) 189–194.
- [6] W.-H. Khoh, J.-D. Hong, Solid-state asymmetric supercapacitor based on manganese dioxide/reduced-graphene oxide and polypyrrole/reduced-graphene oxide in a gel electrolyte, *Colloids Surf. A* 456 (2014) 26–34.
- [7] C. Fu, H. Zhou, R. Liu, Z. Huang, J. Chen, Y. Kuang, Supercapacitor based on electropolymerized polythiophene and multi-walled carbon nanotubes composites, *Mater. Chem. Phys.* 132 (2012) 596–600.
- [8] C. Wu, X. Wang, B. Ju, X. Zhang, L. Jiang, H. Wu, Supercapacitive behaviors of activated mesocarbon microbeads coated with polyaniline, *Int. J. Hydrog. Energy* 37 (2012) 14365–14372.
- [9] X. Sun, G. Wang, H. Sun, F. Lu, M. Yu, J. Lian, Morphology controlled high performance supercapacitor behaviour of the Ni-Co binary hydroxide system, *J. Power Sources* 238 (2013) 150–156.
- [10] K.-J. Jiang, L. Wang, Y.-J. Liu, H.-B. Wang, Y.-M. Liu, L.-L. Wang, Synthesis of polyaniline/2-dimensional graphene analog MoS₂ composites for high-performance supercapacitor, *Electrochim. Acta* 109 (2013) 587–594.
- [11] G.P. Pandey, A.C. Rastogi, Synthesis and characterization of pulsed polymerized poly(3,4-ethylenedioxythiophene) electrodes for high-performance electrochemical capacitors, *Electrochim. Acta* 87 (2013) 158–168.
- [12] J. Li, H. Xie, Y. Li, Fabrication of graphene oxide/polypyrrole nanowire composite for high performance supercapacitor electrodes, *J. Power Sources* 241 (2013) 388–395.
- [13] H. Liu, Y. Wang, X. Gou, T. Qi, J. Yang, Y. Ding, Three-dimensional graphene/polyaniline composite material for high-performance supercapacitor applications, *Mater. Sci. Eng. B* 178 (2013) 293–298.
- [14] K. Liu, Z. Hu, R. Xue, J. Zhang, J. Zhu, Electropolymerization of high stable poly(3,4-ethylenedioxythiophene) in ionic liquids and its potential applications in electrochemical capacitor, *J. Power Sources* 179 (2008) 858–862.
- [15] Y. Li, B. Wang, H. Chen, W. Feng, Improvement of the electrochemical properties via poly(3,4-ethylenedioxythiophene) oriented micro/nanorods, *J. Power Sources* 195 (2010) 3025–3030.
- [16] E. Hür, G.A. Varol, A. Arslan, The study of polythiophene, poly(3-methylthiophene) and poly(3,4-ethylenedioxythiophene) on pencil graphite electrode as an electrode active material for supercapacitor applications, *Synth. Met.* 184 (2013) 16–22.
- [17] E. Hür, A. Arslan, New electrode materials for supercapacitors: pencil graphite electrode coated with cobalt ion doped poly(3-methylthiophene) and poly(3,4-ethylenedioxythiophene), *Synth. Met.* 193 (2014) 81–88.
- [18] C. Arbizani, M.C. Gallazi, M. Mastragostino, M. Rossi, F. Soavi, Capacitance and cycling stability of poly(alkoxythiophene) derivative electrodes, *Electrochim. Commun.* 3 (2001) 16–19.
- [19] A. Laforgue, P. Simon, J.-F. Fauvarque, Chemical synthesis and characterization of fluorinated polyphenylthiophenes: application to energy storage, *Synth. Met.* 123 (2001) 311–319.
- [20] A.S. Sarac, H.-D. Gilsing, A. Gencturk, B. Schulz, Electrochemically polymerized 2,2-dimethyl-3,4-propylenedioxythiophene on carbon fiber for microsupercapacitor, *Prog. Org. Coat.* 60 (2007) 281–286.
- [21] F.Ç. Cebeci, E. Sezer, A.S. Sarac, A novel EDOT-nonbithiazole-EDOT based comonomer as an active electrode material for supercapacitor applications, *Electrochim. Acta* 54 (2009) 6354–6360.
- [22] M. Güllü, Y. Yiğit, A novel asymmetric pseudocapacitor based on poly(5,12-dihydrothieno[3',4':2,3][1,4]dioxino[6,7-b]quinoxaline) coated graphite anode and poly(ethylenedioxythiophene) coated graphite electrode, *Synth. Met.* 162 (2012) 1434–1442.
- [23] M.C. Turhan, A.S. Sarac, A. Gencturk, H.-D. Gilsing, H. Faltz, B. Schulz, Electrochemical impedance characterization and potential dependence of poly[3,4-(2,2-dibutylpropylenedioxy)thiophene] nanostructures on single carbon fiber microelectrode, *Synth. Met.* 162 (2012) 511–515.
- [24] B. Yue, C. Wang, P. Wagner, Y. Yang, X. Ding, D.L. Officer, G.G. Wallace, Electrodeposition of pyrrole and 3-(4-*tert*-butylphenyl)thiophene copolymer for supercapacitor applications, *Synth. Met.* 162 (2012) 2216–2221.
- [25] D. Yiğit, T. Güngör, M. Güllü, Poly(thieno[3,4-b][1,4]dioxine) and poly([1,4]dioxino[2,3-c]pyrrole) derivatives: p- and n- dopable redox-active electrode materials for solid state supercapacitor applications, *Org. Electron.* 14 (2013) 3249–3259.
- [26] E. Ermiş, D. Yiğit, M. Güllü, Synthesis of poly(N-alkyl-3,4-dihydrothieno[3,4-b][1,4]oxazine) derivatives and investigation of their supercapacitive performances for charge storage applications, *Electrochim. Acta* 90 (2013) 623–633.
- [27] A.R. Katritzky, X. Lan, J.Z. Yang, O.V. Denisko, Properties and synthetic utility of N-substituted benzotriazoles, *Chem. Rev.* 98 (1998) 409–548.
- [28] D. Hür, S.F. Ekti Dal, G.A. Varol, E. Hür, N-acylnenzotriazole mediated microwave assisted synthesis of protected and novel unprotected ferrocenoylamidoamino acids, *J. Organomet. Chem.* 696 (2011) 2543–2548.
- [29] S. Saravanan, P.S. Selvan, N. Gopal, J.K. Gupta, B. De, Synthesis and antibacterial activity of some imidazole-5-(4H)one derivatives, *Arch. Pharm. Chem. Life Sci.* 338 (2005) 488–492.
- [30] S.H. Mujawar, S.B. Ambade, T. Battumur, R.B. Ambade, S.-H. Lee, Electropolymerization of aniline on titanium oxide nanotubes for supercapacitor application, *Electrochim. Acta* 56 (2011) 4462–4466.
- [31] M. Jin, G. Han, Y. Chang, H. Zhao, H. Zhang, Flexible electrodes based on polypyrrole/manganese dioxide/polypropylene fibrous membrane composite for supercapacitor, *Electrochim. Acta* 56 (2011) 9838–9845.
- [32] Q. Wang, Q. Cao, X. Wang, B. Jing, H. Kuang, L. Zhou, A high-capacity carbon prepared from renewable chicken feather biopolymer for supercapacitors, *J. Power Sources* 225 (2013) 101–107.
- [33] A. Mirmohseni, M.S. Seyed Dorraji, M.G. Hosseini, Influence of metal oxide nanoparticles on pseudocapacitive behavior of wet-spun polyaniline-multiwall carbon nanotube fibers, *Electrochim. Acta* 70 (2012) 182–192.
- [34] Z. Zhou, D.L. He, R.H. Yang, Y.N. Guo, J.F. Zhong, G.X. Li, Electropolymerization of benzotriazole in room temperature ionic liquid [bmim]PF₆, *J. Appl. Electrochem.* 38 (2008) 1757–1761.
- [35] A. Yağan, N. Özçiçek Pekmez, A. Yıldız, Electropolymerization of poly(N-ethylaniline) on mild steel: synthesis, characterization and corrosion protection, *Electrochim. Acta* 51 (2006) 2949–2955.
- [36] C. Ocampo, R. Oliver, E. Armelin, C. Alemán, F. Estrany, Electrochemical synthesis of poly(3,4-ethylenedioxythiophene) on steel electrodes: properties and characterization, *J. Polym. Res.* 13 (2006) 193–200.
- [37] E. Frackowiak, F. Béguin, Carbon materials for the electrochemical storage of energy in capacitors, *Carbon* 39 (2001) 937–950.
- [38] T.P. Gujar, W.-Y. Kim, I. Puspitasari, K.-D. Jung, O.-S. Joo, Electrochemically deposited nanograin ruthenium oxide as a pseudocapacitive electrode, *Int. J. Electrochem. Sci.* 2 (2007) 666–673.
- [39] R.K. Sharma, L. Zhai, Multiwall carbon nanotube supported poly(3,4-ethylenedioxythiophene)/manganese oxide nano-composite electrode for supercapacitors, *Electrochim. Acta* 54 (2009) 7148–7155.
- [40] D.S. Dhawale, A. Vinu, C.D. Lokhande, Stable nanostructured polyaniline electrode for supercapacitor application, *Electrochim. Acta* 56 (2011) 9482–9487.
- [41] D.P. Dubal, C.D. Lokhande, Significant improvement in the electrochemical performances of nano-nest like amorphous MnO₂ electrodes due to Fe doping, *Ceram. Int.* 39 (2013) 415–423.
- [42] D.P. Dubal, R. Holze, All-solid-state flexible thin film supercapacitor based on Mn₂O₄ stacked nanosheets with gel electrolyte, *Energy* 51 (2013) 407–412.
- [43] K. Lota, V. Khomenko, E. Frackowiak, Capacitance properties of poly(3,4-ethylenedioxythiophene)/carbon nanotubes composites, *J. Phys. Chem. Solids* 65 (2004) 295–301.
- [44] D.P. Dubal, W.B. Kim, C.D. Lokhande, Galvanostatically deposited Fe: MnO₂ electrodes for supercapacitor application, *J. Phys. Chem. Solids* 73 (2012) 18–24.
- [45] H. Heli, H. Yadegari, A. Jabbari, Graphene nanosheets-poly(o-aminophenol) nanocomposite for supercapacitor applications, *Mater. Chem. Phys.* 134 (2012) 21–25.
- [46] G.A. Snook, P. Kao, A.S. Best, Conducting-polymer-based supercapacitor devices and electrodes, *J. Power Sources* 196 (2011) 1–12.
- [47] P. Sen, A. De, Electrochemical performances of poly(3,4-ethylenedioxythiophene)-NiFe₂O₄ nanocomposite as electrode for supercapacitor, *Electrochim. Acta* 55 (2010) 4677–4684.
- [48] C. Lei, P. Wilson, C. Lekakou, Effect of poly(3,4-ethylenedioxythiophene) (PEDOT) in carbon-based composite electrodes for electrochemical capacitors, *J. Power Sources* 196 (2011) 7823–7827.
- [49] B. Yue, C. Wang, X. Ding, G.C. Wallace, Polypyrrole coated nylon lycra fabric as stretchable electrode for supercapacitor applications, *Electrochim. Acta* 68 (2012) 18–24.